



Published in final edited form as:

NMR Biomed. 2015 November ; 28(11): 1589–1597. doi:10.1002/nbm.3427.

Evaluation of skeletal muscle DTI in patients with Duchenne Muscular Dystrophy

M.T. Hooijmans¹, B.M. Damon², M. Froeling³, M.J. Versluis⁴, J. Burakiewicz¹, J.J.G.M Verschuuren⁵, A.G. Webb¹, E.H. Niks⁵, and H.E. Kan¹

¹Dept of Radiology, C.J. Gorter Center for High Field MRI, Leiden University Medical Centre, Leiden, The Netherlands ²Depts. of Radiology and Radiological Sciences, Biomedical Engineering, and Molecular Physiology and Biophysics, Vanderbilt University, Nashville TN USA ³Dept of Radiology, Utrecht Medical Center, Utrecht, The Netherlands ⁴Philips Healthcare, Benelux, Netherlands ⁵Dept of Neurology, Leiden University Medical Centre, Leiden, The Netherlands

Keywords

Diffusion Tensor Imaging; Signal to Noise Ratio; fat fraction; mean water T₂; Duchenne Muscular Dystrophy

Introduction

Spin-echo-based diffusion tensor imaging (DTI) is an intrinsically T₂-weighted method to measure the apparent diffusion of water molecules in tissue. Water diffusion can be hindered by structures such as mitochondria, sarcoplasmic reticulum, macromolecules and the cell membrane. (1) DTI is commonly used as a non-invasive and quantitative method to assess fiber organization in healthy, diseased and damaged skeletal muscle. (2–8) Changes in DTI parameters have been observed with respect to age, gender, injury, disease and exercise, as well as between individual muscles, showing the potential of DTI as a measure for overall muscle quality. (9–15) DTI has also been used to assess changes in fiber type distributions, to monitor muscle recovery after marathon running, and to discriminate between different phases of the recovery after artery ligation. (16–19) As DTI is a quantitative technique, high quality data are necessary to obtain reliable estimates of DTI based parameters. Even in healthy muscle tissue it is challenging to achieve high signal-to-noise-ratio (SNR) due to the tissue's short T₂, long T₁, and a relatively high diffusivity of water. Recently, several simulation studies have shown that the reliability of estimating DTI parameters is substantially affected by the SNR, water T₂ value, and percentage fat composition (%fat) (20–22). These simulation studies predicted that low SNR data result in an overestimation of fractional anisotropy (FA) and an underestimation of the three eigenvalues (λ_1 , λ_2 , λ_3) and

Corresponding author: M.T. Hooijmans, Department of Radiology, C-03-Q, LUMC, Albinusdreef 2, 2333 ZA LEIDEN, Phone: +31-71-5265411, Fax: +31-72-5268256, m.t.hooijmans@lumc.nl.

Financial disclosures: All other authors have nothing to declare.

mean diffusivity (MD). (20, 22) Increases in T_2 , often associated with muscle damage, may indirectly affect the diffusion parameters due to the associated increase in SNR. (20, 22) In addition, the increases in fat % associated with age and pathology may alter the diffusion parameters due to increased partial volume effects. (21, 22) DMD is an X-linked disease caused by a mutation in the dystrophin gene, and is characterized by progressive muscle weakness and muscle damage. (23) In many muscular dystrophies, muscles show structural changes such as fat infiltration and fibrosis that increase with age, as well as oedema and/or inflammatory processes which increase the mean water T_2 . (24–26) As a result, true differences in DTI measurements in this population may be obscured by MR confounders such as increased fat fraction and increased T_2 . The majority of previous skeletal muscle DTI studies have focused on its properties as a non-invasive and quantitative method to assess differences in microstructural organization and on performing fiber tractography. However, the potential role that confounders such as SNR, %fat and water T_2 values could have on the detected differences in DTI parameters in healthy and diseased muscle has not been addressed experimentally in patients with a muscle disease. The overall purpose of this study was to acquire skeletal muscle DTI measurements in patients with DMD and healthy controls, combined with measurements to assess mean water T_2 , %fat and SNR for an in-vivo evaluation of their effect on the DTI measurements. Furthermore, DTI was used as a non-invasive and quantitative method to assess changes in DTI parameters between these groups. Finally, the feasibility of ascribing these changes to pathology or confounding effects using multi-parametric MRI was assessed. As such we obtained data in a group of DMD patients and age-matched healthy controls and looked at the differences in DTI parameters between groups.

Methods

Study population

Twenty-one DMD patients (9.5 ± 3.1 yrs; range, 5–16 yrs) and 12 age-matched healthy controls (9.7 ± 2.9 yrs, range: 5–14 yrs) participated in the study. The DMD patients were recruited from the Dutch Dystrophinopathy Database, while the controls were recruited from local schools. The diagnosis DMD was confirmed by a mutation in the DMD gene and lack of dystrophin expression in the muscle biopsy. Of the 21 DMD patients, 8 were wheelchair bound, 13 were fully ambulant and all boys used corticosteroids. The study was approved by the local medical ethics committee. All participants or their legal representatives signed informed consent.

MR examination

MR datasets of the right lower leg were acquired on a 3T MR scanner (Ingenia, Philips, Best, Netherlands) with a 32-element anterior body receive coil. Patients were positioned in a feet-first supine position in the scanner. The total duration of the scan was 25 minutes and contained:

- i. a SE-EPI DTI sequence to obtain DTI parameters (TR/TE 2990/49 ms; number of signal averages (NSA) 6; number of gradient directions 16; b-value 0,450 s/mm²; voxel size 2×2×6 mm; 12 contiguous slices; half scan 0.7; SENSE factor in RL

direction; spectrally adiabatic inversion recovery (SPAIR) and slice-selection gradient reversal (SSGR) fat suppression on the aliphatic fat peak with spectrally selective suppression of the olefinic fat peak;

- ii. SE-EPI without diffusion weighting to determine the SNR (TR/TE 3020/49 ms; NSA 6; b-value 0 s/mm²; voxel size 2×2×6 mm; 12 contiguous slices; 10 dynamics, SPAIR and SSGR fat suppression on the aliphatic fat and selective suppression of the olefinic fat peak) (21);
- iii. TSE T₁-weighted images for anatomical reference (TR/TE 630/30ms; voxel size 1.5×1.5×6 mm; no gap, 12 slices),
- iv. Three point Dixon images to determine the amount of fat infiltration (TR/TE/ TE 210/4.41/0.76 ms; NSA 2; flip angle 8°; voxel size 1×1×10 mm; slice gap 5 mm; 23 slices)
- v. Multi turbo spin echo sequence to measure the water T₂ relaxation time (17 echoes; TR/TE/ TE 3000/8/8 ms; refocussing angle 180°; voxel size 1.4×1.8×10 mm; slice gap 20 mm;; 5 slices, no fat suppression).

Data-analysis

DTI-analysis was performed using a custom-built toolbox in Mathematica (5, 27). Data were de-noised, registered and corrected for eddy currents before the tensor calculation and estimation of the individual eigenvalues ($\lambda_1, \lambda_2, \lambda_3$), mean diffusivity (MD) and the fractional anisotropy (FA). (5) A Weighted-Linear-Least-Squares (WLLS) method was used for tensor calculation and MD and FA were determined with standard equations using these eigenvalues. A separate SE-EPI sequence with 10 dynamics was used to assess the SNR, which was defined as the mean signal over the 10 dynamics divided by the standard deviation over the same 10 dynamics. The SNR was determined per pixel and presented as a mean of all pixels within a region of interest (ROI), as described below. The determination of the water T₂-relaxation times used a tri-exponential fitting routine written in MATLAB based on a previously described method (28). Quantitative fat fractions were calculated as signal intensity (SI) fat/ (SI fat+ SI water)*100 from the 3-point Dixon images. Fat and water images were generated using a multi-peak model based on a six fat peak spectrum. Values were not corrected for T₂* relaxation effects. Even though the relaxation between the echoes is small in tissues with no significant iron concentrations, this could have resulted in a small overestimation of fat fractions in the low fat ranges (29). Subsequently, the sequence was optimized with respect to TR and flip angle to minimize T₁ relaxation effects. ROIs were manually drawn for the 3P-Dixon, MSE and the T₁-weighted sequence, using Medical Image Processing, Analysis and Visualization (MIPAV) software (<http://mipav.cit.nih.gov>) for six individual lower leg muscles: the lateral head of the gastrocnemius (GL), medial head of the gastrocnemius (GM), soleus (SOL), tibialis anterior (TA), peronei (PER) and the tibialis posterior (TP) muscles (Figure 1f). Boundaries of the ROIs were identified to always fall within a muscle in order to avoid contamination of subcutaneous fat and fatty septa between muscles. The ROIs from the T₁-weighted images were used for anatomical reference in the DTI and SNR assessments. All outcome measures are reported as a mean value of all pixels within a ROI over multiple slices. Because of sequence-specific

differences in slice thickness, the number of slices used in the analysis varied between sequences. However, all sequences covered the same volume of tissue as the DTI sequence.

Simulations

Simulations were performed according to Froeling et al. (20) and Damon et al. (22). For the simulations the parameters were set identical to the MRI experiments (TE = 49 ms, TR = 2990 ms, 16 gradient directions and $b = 450 \text{ s/mm}^2$). The fat compartment was simulated using $T_2 = 80/550 \text{ ms}$ with a ratio of 2:1, $T_1 = 300 \text{ ms}$, proton density $\rho = 0.1$ and MD = 0.6 mm²/2 and FA=0. For the muscle compartment $T_2 = 37 \text{ ms}$ (the mean of all muscles), $T_1 = 1200 \text{ ms}$ and $\rho = 0.8$ were used. Two simulation experiments were performed: simulation 1 - diffusion parameters as a function of SNR, simulation2 - diffusion parameters as a function of the fat fraction. The muscle diffusion properties were set to values estimated from the normal distribution given by all muscles of healthy subjects with an SNR > 25 and from all muscles of Duchene patients with a fat fraction < 10%, for simulation 1 and 2 respectively. The fat fractions and the SNR was also estimated from the same subsets for each simulation. For each SNR value, ranging from 1 to 55 with steps of 2, and for each fat fraction, ranging from 0 to 60 % with steps of 2 %, 5000 virtual subjects were simulated by generating a noisy diffusion signal using randomly selected values using the previously determined normal distributions of the diffusion properties, SNR and fat fraction using,

$$S(\rho, T_1, T_2, TR, TE) = \rho \cdot (1 - e^{-TR/T_1}) \cdot e^{-TE/T_2}, \text{ and}$$

$$S(b, \vec{g}) = f \cdot S_{fat}(\rho_{fat}, T_{1,fat}, T_{2,fat}, TR, TE) \cdot e^{-b \vec{g} \mathbf{D}_{fat} \vec{g}^T}$$

$$+ (1 - f) \cdot S_{mus}(\rho_{mus}, T_{1,mus}, T_{2,mus}, TR, TE) \cdot e^{-b \vec{g} \mathbf{D}_{mus} \vec{g}^T} + \varepsilon$$

where $S(b, \vec{g})$ is the noisy diffusion signal for b-value b and gradient direction \vec{g} , f is the fat fraction, ρ the proton density, T_1 and T_2 the longitudinal and transvers magnetization, ε the Rician noise signal and \mathbf{D}_{fat} and \mathbf{D}_{mus} the diffusion tensors for fat and muscle respectively. The simulated signal was then used to calculate the distribution of diffusion parameters as a function of SNR and fat.

Statistical Analysis

The Pearson correlation coefficient was used to evaluate the correlation between SNR, %fat and muscle T_2 value and the estimation of the individual DTI parameters. The evaluation of SNR involved datasets of healthy controls only. The evaluation of the effect of %fat on the DTI estimation involved data-sets of DMD patients with an SNR>20 only, so as to evaluate better the separate effects of SNR and %fat. To determine the effect of mean water T_2 on the DTI parameters and SNR, datasets of both groups were evaluated individually, as DMD patients are known to have an elevated T_2 . A general linear model was used to assess differences in DTI-parameters and mean water T_2 between patients with DMD and healthy controls. The water T_2 was included as a covariate for the DTI parameters and a Fischer least significant difference (LSD) model was used to correct for multiple comparisons. The between-group analysis was performed twice, once with only datasets with an SNR>20 and once with all data-sets taking into account the effect of confounders. The significance level

was set at $p < 0.05$. All statistical analyses were performed using SPSS version 20 for Windows (SPSS Inc., Chicago).

Results

All scans were successfully performed in DMD patients and healthy controls. Example multi-contrast images are illustrated in Figure 1.

The effect of SNR

Mean SNR values averaged over all muscles were 27.9 ± 9.8 in healthy controls (HC) and 20.9 ± 9.7 in DMD patients. The associations between DTI parameters and SNR are visualized in Figure 2(A–E). In the low SNR ranges, MD and the eigenvalues are underestimated and FA is overestimated. Values of FA ($r = -0.35$, $p < 0.001$), λ_1 ($r = -0.52$, $p < 0.001$) and λ_2 ($r = -0.28$, $p < 0.049$) were negatively correlated with SNR; no significant correlation was observed for λ_3 . For the majority of the DTI-parameters stabilization of the values occurred at SNR levels above 20. Eliminating data points below this threshold would result in exclusion of 18% (13/72) of the total healthy control ROI's and an exclusion of 47% (93/198) of the total ROIs. Twelve of the excluded HC ROIs belonged to two subjects. However, it should also be noted that correlations between MD ($r = -0.38$, $p = 0.029$), λ_1 ($r = -0.54$, $p < 0.0001$) and λ_2 ($r = -0.19$, $p = 0.0175$) and SNR remained even when ROIs with an SNR < 20 were excluded. Furthermore, similar behaviour is visualized with the simulation experiment, describing the diffusion parameters as a function of SNR, in which almost all in-vivo obtained data points fall within one standard deviation of the simulated signal, see Figure 2(A–E).

The effect of fat fraction

The mean %fat of all lower leg muscles was $17.4\% \pm 14.4\%$ in DMD patients and $4.3\% \pm 0.8\%$ in healthy controls. Only datasets of DMD patients with an SNR above 20 were included in this part of the analysis, as healthy controls normally do not show fat infiltration. All data points are visualized in Figure 3 (A–E) and show a decrease as was also seen in the simulation experiment, except for the FA which tends to show the opposite behaviour (Fig. 3 A–E). Significant negative correlations were observed for MD ($r = -0.26$, $p = 0.04$) and λ_3 ($r = -0.34$, $p = 0.02$) and no correlations were present for FA, λ_1 and λ_2 in the in-vivo data.

The effect of mean water T_2 relaxation times

In all lower leg muscle, the mean water T_2 was significantly greater in the DMD patients than in the healthy controls ($p < 0.001$). Mean water T_2 values, averaged over all the muscles, were 39.5 ± 0.6 ms for DMD patients and 35.1 ± 0.5 ms for healthy controls. Correlations between mean water T_2 and the DTI parameters were assessed per group individually. For both groups no correlations were observed between the mean water T_2 and the individual DTI-parameters (Figures 4A–E). Additionally, the correlation between mean water T_2 and SNR was assessed and no significant correlations were found.

Assessing differences in DTI parameters between groups

Including all ROIs—Table 1 lists the mean diffusion values per muscle of the DMD patients and healthy controls using all ROIs. Between-group analysis without data selection based on the confounders showed a significant increase in MD ($p=0.020$, Fig. 5A) and λ_3 ($p=0.024$) in the TA muscle for DMD patients compared to healthy controls. Also, a significant increase in FA was found in the GL ($p=0.04$), SOL ($p=0.006$) and PER ($p=0.049$) muscles (Fig. 5C, Table. 1). No significant changes in λ_1 and λ_2 were observed between groups.

Including ROIs with SNR>20—Mean and standard deviations of the DTI parameters per muscle of the DMD patients and healthy controls using only ROIs with SNR>20 are shown in table 1. Taking only ROIs with an SNR>20, a total of 47% (93/198) of the ROIs were excluded from the between-group analysis. Group comparison now showed a significantly increased MD in the TA muscle ($p<0.009$) (Fig. 5B) together with a significantly higher λ_3 in the GL ($p<0.001$) and TA muscle ($p<0.007$) for DMD patients compared to healthy controls (Fig. 5B). No significant changes between groups were detected in λ_1 and λ_2 (Table. 1). These results are in accordance with the group analysis using all images. However, in contrast to the previous group analysis, no significant changes were detected for FA. Although not significantly different, some trends were observed towards a lower FA in the TA ($p=0.059$) and TP muscle ($p=0.058$, Fig. 5D), increased λ_2 in the TA muscle ($p=0.063$) and an increased λ_1 in the SOL muscle ($p=0.084$) of DMD patients.

Discussion

In this study we evaluated the effect of individual confounders on the DTI-parameter estimation in patients with DMD and healthy controls. In line with the conclusions of previous simulation-based works (20–22), both SNR and %fat influenced DTI-parameter estimation. In contrast, the significantly elevated mean water T_2 had no effect on the DTI parameter estimation in patients with DMD. When all data-sets were included in the between-group analysis, there were between-group differences in more individual DTI parameters (FA, MD and λ_3) than when only datasets with sufficient SNR (SNR>20) were used (MD and λ_3). Because the number of statistically significant findings is reduced when low SNR data are eliminated, at least some of the between-group differences in DTI parameters are most likely to have been caused by confounding factors. Overall, these findings support the conclusion that distinguishing between the causes of changes in DTI measures in skeletal muscle requires in vivo measurements of SNR, mean water T_2 and % fat.

SNR as a confounding parameter

The stabilization effect visualized in our distributions in the high SNR ranges, together with the overestimation of FA and the underestimation of MD and the eigenvalues in the low SNR ranges, are in line with our simulation experiment as well as with previous work. (20, 22) In a low SNR condition, an erroneously elevated measurement of anisotropy can occur even in highly isotropic structures. (30) This previously reported phenomenon underlies the behaviour visible in the distributions of the DTI-parameters plotted against SNR. (31) In

could be due to the presence of confounding effects on the DTI measurements. As both low SNR and high %fat datasets are included in this part of the group analysis, it is most likely that the apparent increases in FA simply reflect low SNR, rather than changes in muscle microstructure. This conclusion is supported by previous experimental work that showed that FA is artificially increased in regions with significant fat-muscle partial volume artefacts. (21) However, the significantly increased MD and λ_3 in the TA muscle and the lack of any significant changes in MD or the eigenvalues in the other muscles are inconsistent with the effects predicted by low SNR and high fat levels. (2, 32) One possible explanation for these elevated diffusivities in the TA is that the effect of pathology may be much stronger than the potential effect of confounders. Second, it might be that the estimation of MD and the eigenvalues – particularly when using WLLS for tensor estimation – is slightly less sensitive to the influence of noise. This is consistent with the prediction of simulation-based work. (20) Finally, it could be that MD and the eigenvalues are only affected in the higher fat fractions and that this DMD cohort did not contain many patients with highly fat infiltrated muscles.

Between-Group Differences Determined by using only ROIs with SNR>20

After accounting for SNR as a confounding effect, using only datasets with a SNR cut-off above 20, micro-structural changes are observed between groups. A significant increase in MD in the TA and increases in λ_3 in the TA and GL muscle of DMD patients were found. In contrast to the observations in the between-group analysis using all datasets, no significant increases in FA were detected between groups when correcting for low SNR. As this between-group analysis is based on a smaller number of subjects than the analysis using all ROIs, this could have resulted in not finding changes in FA. This is in accordance with mouse skeletal muscle work where increases in MD and λ_3 have been reported as an immediate response to muscle injury. (17) At the same time, the observed trend for a decrease in FA combined with the increase in MD in the TA muscle is in agreement with common changes associated with muscle injury and damage. (2, 4, 17, 33, 34) However, as a consequence of not fully correcting for confounders it could be that both %fat and SNR have had a potential effect on the DTI parameter estimation. As the effect of both confounders would result in an underestimation of MD and λ_3 , it is likely that the observed changes in these DTI measures, in both between group analysis, are due to changes in the intrinsic diffusion rather than due to confounding effects. Therefore, the increased MD and λ_3 in the TA muscle is most likely reflecting the pathophysiology in patients with DMD.

Previous studies

Besides the agreements found with clinical applications in diseased and damaged human skeletal muscle, there is to our knowledge one other clinical study which focused on skeletal muscle DTI in patients with DMD; that study reported a significantly increased FA and decreased MD with disease progression. (9, 32) These observations are to some extent in line with the results from our group analysis using all ROIs, to be precise with the detected significant increased FA in several muscles, which is likely caused by confounders, as both %fat and low SNR result in an overestimation of FA: no corrections for the confounding effects of SNR, %fat or T_2 changes were made.

Limitations

A few potential limitations of the study should be acknowledged. First of all, no distinction has been made between the six individual muscles during the evaluation of confounding effects on the DTI parameter estimation. All evaluations are based on the assumption that variations in DTI parameters between muscles are negligible. (35) As previous studies have shown that the variations between muscles are minor compared to the changes detected due to confounding effects, we assume that these small variations between muscles will be outweighed by the larger effects of SNR, % fat and T_2 changes. (35) Secondly, as mentioned before a large amount of data has been excluded to retain quality for the between-group analysis using only ROIs with $SNR > 20$. This could potentially have resulted in not finding any differences in some of the DTI measures between the groups. A larger number of subjects, combined with an even further optimized DTI protocol, will be advisable for future work. Lastly, the tri-exponential T_2 fitting method has not yet been shown to produce equivalent water T_2 estimates to fat-suppressed T_2 methods. In using this method, we are assuming that the effects of the confounding parameters on the DTI estimates are greater than any error or variability produced by using the tri-exponential fitting approach.

Conclusion

In conclusion, experimental evaluation of the effects of SNR, %fat and mean water on the DTI measurements showed that a sufficient SNR is essential for a reliable estimation of the DTI parameters in skeletal muscle and that in vivo measurements of % fat and mean water T_2 are necessary to assess whether detected changes in DTI parameters could be ascribed to pathophysiology or to confounding effects. Overall, our work suggests that reliable DTI measurements in skeletal muscle can be obtained in DMD patients and healthy controls, while accounting for confounding factors.

Acknowledgments

Grant: This work was funded the Netherlands Organization for Health Research and Development (ZonMW) (grant number 113302001). Bruce Damon was supported by NIH/NIAMS R01 AR050101.

MH, BD, MF, JB and HK were part of Working group 3 (WG3): "Explore new contrasts, targets and imaging techniques for NMD", MYO-MRI COST-Action (BM1304), "Applications of MR imaging and spectroscopy techniques in neuromuscular disease: collaboration on outcome measures and pattern recognition for diagnostics and therapy development," European Cooperation in Science and Technology (COST).

JV and EN report trial support from Biomerin, GSK, Lilly and Santhera, outside the submitted work. JV reports consultancy for Prosensa. HK reports consultancy for aTyr pharma, outside the submitted work. All reimbursements were received by the LUMC. No personal financial benefits were received.

List of abbreviations

DMD	Duchenne muscular dystrophy
SD	Standard deviation
GL	Lateral head of Gastrocnemius muscle
GM	Medial head of Gastrocnemius muscle

PER	Peroneus muscle
SOL	Soleus muscle
TA	Anterior Tibialis muscle
TP	Posterior Tibialis muscle
MD	Mean Diffusivity
FA	Fractional Anisotropy
λ_1	Lambda 1 (principal eigenvalue)
λ_2	Lambda 2 (second eigenvalue)
λ_3	Lambda 3 (third eigenvalue)
SNR	Signal-to-Noise Ratio
DTI	Diffusion Tensor Imaging
ROI	Region of Interest
%fat	Fat percentage

References

1. Cleveland GG, Chang DC, Hazlewood CF, Rorschach HE. Nuclear magnetic resonance measurement of skeletal muscle: anisotropy of the diffusion coefficient of the intracellular water. *Biophys J*. 1976; 16(9):1043–1053. [PubMed: 963204]
2. Qi J, Olsen NJ, Price RR, Winston JA, Park JH. Diffusion-weighted imaging of inflammatory myopathies: polymyositis and dermatomyositis. *J Magn Reson Imaging*. 2008; 27(1):212–217. [PubMed: 18022843]
3. Kermarrec E, Budzik JF, Khalil C, Le TV, Hancart-Destee C, Cotten A. In vivo diffusion tensor imaging and tractography of human thigh muscles in healthy subjects. *AJR Am J Roentgenol*. 2010; 195(5):W352–W356. [PubMed: 20966300]
4. Zaráiskaya T, Kumbhare D, Noseworthy MD. Diffusion tensor imaging in evaluation of human skeletal muscle injury. *J Magn Reson Imaging*. 2006; 24(2):402–408. [PubMed: 16823776]
5. Froeling M, Nederveen AJ, Heijtel DF, Lataster A, Bos C, Nicolay K, Maas M, Drost MR, Strijkers GJ. Diffusion-tensor MRI reveals the complex muscle architecture of the human forearm. *J Magn Reson Imaging*. 2012; 36(1):237–248. [PubMed: 22334539]
6. Sinha S, Sinha U, Edgerton VR. In vivo diffusion tensor imaging of the human calf muscle. *J Magn Reson Imaging*. 2006; 24(1):182–190. [PubMed: 16729262]
7. Budzik JF, Balbi V, Verclytte S, Pansini V, Le TV, Cotten A. Diffusion tensor imaging in musculoskeletal disorders. *Radiographics*. 2014; 34(3):E56–E72. [PubMed: 24819802]
8. Budzik JF, Le TV, Demondion X, Morel M, Chechin D, Cotten A. In vivo MR tractography of thigh muscles using diffusion imaging: initial results. *Eur Radiol*. 2007; 17(12):3079–3085. [PubMed: 17639406]
9. Ponrartana S, Ramos-Platt L, Wren TA, Hu HH, Perkins TG, Chia JM, Gilsanz V. Effectiveness of diffusion tensor imaging in assessing disease severity in Duchenne muscular dystrophy: preliminary study. *Pediatr Radiol*. 2014
10. van Donkelaar CC, Kretzers LJ, Bovendeerd PH, Lataster LM, Nicolay K, Janssen JD, Drost MR. Diffusion tensor imaging in biomechanical studies of skeletal muscle function. *J Anat*. 1999; 194(Pt 1):79–88. [PubMed: 10227669]
11. Sinha U, Csapo R, Malis V, Xue Y, Sinha S. Age-related differences in diffusion tensor indices and fiber architecture in the medial and lateral gastrocnemius. *J Magn Reson Imaging*. 2014

12. Scheel M, Prokscha T, von RP, Winkler T, Dietrich R, Bierbaum S, Arampatzis A, Diederichs G. Diffusion tensor imaging of skeletal muscle--correlation of fractional anisotropy to muscle power. *Rofo*. 2013; 185(9):857–861. [PubMed: 23888473]
13. Okamoto Y, Kunimatsu A, Kono T, Nasu K, Sonobe J, Minami M. Changes in MR diffusion properties during active muscle contraction in the calf. *Magn Reson Med Sci*. 2010; 9(1):1–8. [PubMed: 20339260]
14. Galban CJ, Maderwald S, Uffmann K, Ladd ME. A diffusion tensor imaging analysis of gender differences in water diffusivity within human skeletal muscle. *NMR Biomed*. 2005; 18(8):489–498. [PubMed: 16075414]
15. Damon BM, Ding Z, Anderson AW, Freyer AS, Gore JC. Validation of diffusion tensor MRI-based muscle fiber tracking. *Magn Reson Med*. 2002; 48(1):97–104. [PubMed: 1211936]
16. Froeling M, Oudeman J, Strijkers GJ, Maas M, Drost MR, Nicolay K, Nederveen AJ. Muscle Changes Detected by Diffusion-Tensor Imaging after Long-Distance Running. *Radiology*. 2014:140702.
17. Heemskerk AM, Strijkers GJ, Drost MR, van Bochove GS, Nicolay K. Skeletal muscle degeneration and regeneration after femoral artery ligation in mice: monitoring with diffusion MR imaging. *Radiology*. 2007; 243(2):413–421. [PubMed: 17384238]
18. Scheel M, von RP, Winkler T, Arampatzis A, Prokscha T, Hamm B, Diederichs G. Fiber type characterization in skeletal muscle by diffusion tensor imaging. *NMR Biomed*. 2013; 26(10):1220–1224. [PubMed: 23553895]
19. Okamoto Y, Mori S, Kujiraoka Y, Nasu K, Hirano Y, Minami M. Diffusion property differences of the lower leg musculature between athletes and non-athletes using 1.5T MRI. *MAGMA*. 2012; 25(4):277–284. [PubMed: 22086307]
20. Froeling M, Nederveen AJ, Nicolay K, Strijkers GJ. DTI of human skeletal muscle: the effects of diffusion encoding parameters, signal-to-noise ratio and T2 on tensor indices and fiber tracts. *NMR Biomed*. 2013; 26(11):1339–1352. [PubMed: 23670990]
21. Williams SE, Heemskerk AM, Welch EB, Li K, Damon BM, Park JH. Quantitative effects of inclusion of fat on muscle diffusion tensor MRI measurements. *J Magn Reson Imaging*. 2013; 38(5):1292–1297. [PubMed: 23418124]
22. Damon BM. Effects of image noise in muscle diffusion tensor (DT)-MRI assessed using numerical simulations. *Magn Reson Med*. 2008; 60(4):934–944. [PubMed: 18816814]
23. Hoffman EP, Brown RH Jr, Kunkel LM. Dystrophin: the protein product of the Duchenne muscular dystrophy locus. *Cell*. 1987; 51(6):919–928. [PubMed: 3319190]
24. Sarkozy A, Deschauer M, Carlier RY, Schrank B, Seeger J, Walter MC, Schoer B, Reilich P, Leturq F, Radunovic A, Behin A, Laforet P, Eymard B, Schreiber H, Hicks D, Vaidya SS, Glaser D, Carlier PG, Bushby K, Lochmuller H, Straub V. Muscle MRI findings in limb girdle muscular dystrophy type 2L. *Neuromuscul Disord*. 2012; 22(Suppl 2):S122–S129. [PubMed: 22980763]
25. Janssen BH, Voet NB, Nabuurs CI, Kan HE, de Rooy JW, Geurts AC, Padberg GW, van Engelen BG, Heerschap A. Distinct disease phases in muscles of facioscapulohumeral dystrophy patients identified by MR detected fat infiltration. *PLoS One*. 2014; 9(1):e85416. [PubMed: 24454861]
26. Wokke BH, Hooijmans MT, van den Bergen JC, Webb AG, Verschuuren JJ, Kan HE. Muscle MRS detects elevated PDE/ATP ratios prior to fatty infiltration in Becker muscular dystrophy. *NMR Biomed*. 2014; 27(11):1371–1377. [PubMed: 25196814]
27. Froeling M, Oudeman J, van den Berg S, Nicolay K, Maas M, Strijkers GJ, Drost MR, Nederveen AJ. Reproducibility of diffusion tensor imaging in human forearm muscles at 3.0 T in a clinical setting. *Magn Reson Med*. 2010; 64(4):1182–1190. [PubMed: 20725932]
28. Azzabou N, Loureiro de SP, Caldas E, Carlier PG. Validation of a generic approach to muscle water T2 determination at 3T in fat-infiltrated skeletal muscle. *J Magn Reson Imaging*. 2014
29. Loughran T, Higgins DM, McCallum M, Coombs A, Straub V, Hollingsworth KG. Improving highly accelerated fat fraction measurements for clinical trials in muscular dystrophy: origin and quantitative effect of R2* changes. *Radiology*. 2015; 275(2):570–578. [PubMed: 25575118]
30. Basser PJ, Pajevic S. Statistical artifacts in diffusion tensor MRI (DT-MRI) caused by background noise. *Magn Reson Med*. 2000; 44(1):41–50. [PubMed: 10893520]

31. Basser PJ, Pierpaoli C. Microstructural and physiological features of tissues elucidated by quantitative-diffusion-tensor MRI. *J Magn Reson B*. 1996; 111(3):209–219. [PubMed: 8661285]
32. Ponrartana S, Andrade KE, Wren TA, Ramos-Platt L, Hu HH, Bluml S, Gilsanz V. Repeatability of chemical-shift-encoded water-fat MRI and diffusion-tensor imaging in lower extremity muscles in children. *AJR Am J Roentgenol*. 2014; 202(6):W567–W573. [PubMed: 24848851]
33. Heemkerk AM, Drost MR, van Bochove GS, van Oosterhout MF, Nicolay K, Strijkers GJ. DTI-based assessment of ischemia-reperfusion in mouse skeletal muscle. *Magn Reson Med*. 2006; 56(2):272–281. [PubMed: 16826605]
34. Qin EC, Juge L, Lambert SA, Paradis V, Sinkus R, Bilston LE. In Vivo Anisotropic Mechanical Properties of Dystrophic Skeletal Muscles Measured by Anisotropic MR Elastographic Imaging: The mdx Mouse Model of Muscular Dystrophy. *Radiology*. 2014; 273(3):726–735. [PubMed: 25105354]
35. Li K, Dortch RD, Welch EB, Bryant ND, Buck AK, Towse TF, Gochberg DF, Does MD, Damon BM, Park JH. Multi-parametric MRI characterization of healthy human thigh muscles at 3.0 T - relaxation, magnetization transfer, fat/water, and diffusion tensor imaging. *NMR Biomed*. 2014; 27(9):1070–1084. [PubMed: 25066274]

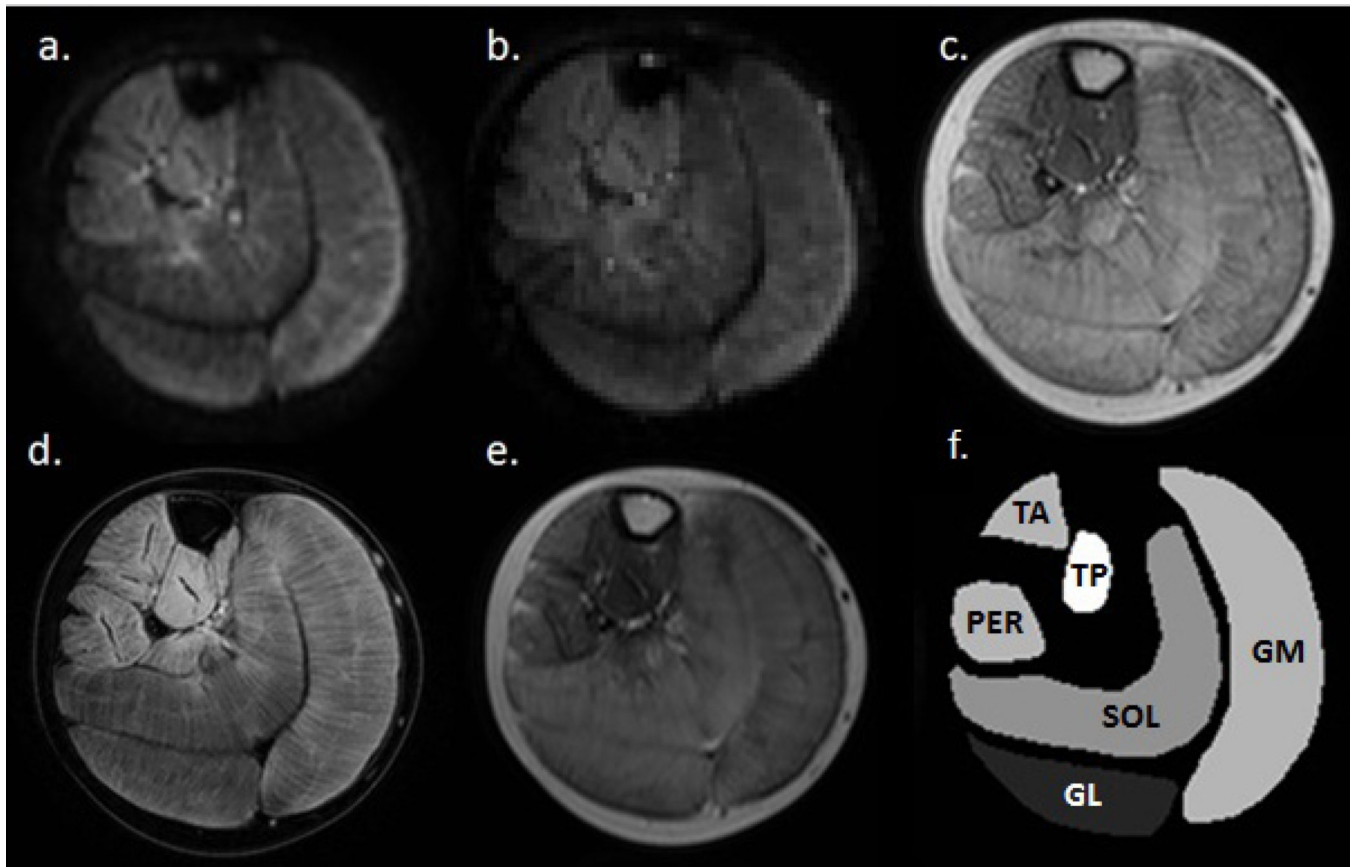


Figure 1.

Axial multi-parametric images of the lower leg of a DMD patient: a fat-suppressed diffusion weighted SE-EPI image (b-value of 450 mm/s²) (a); a fat-suppressed SE-EPI image without diffusion weighting (b); T₁-weighted image; (c) a 3-point Dixon water image; (d) the 7th echo of a multi-spin-echo image (TE: 56 ms); (e) and a representation of the masks created for the 6 lower leg muscles - medial and lateral head of gastrocnemius (GM, GL), soleus (SOL), anterior tibialis (TA), peroneus (PER) and posterior tibialis (TP)) (f). Note the complete suppression of the fat signal in (a) and (b), resulting from the use of the combined fat suppression method.

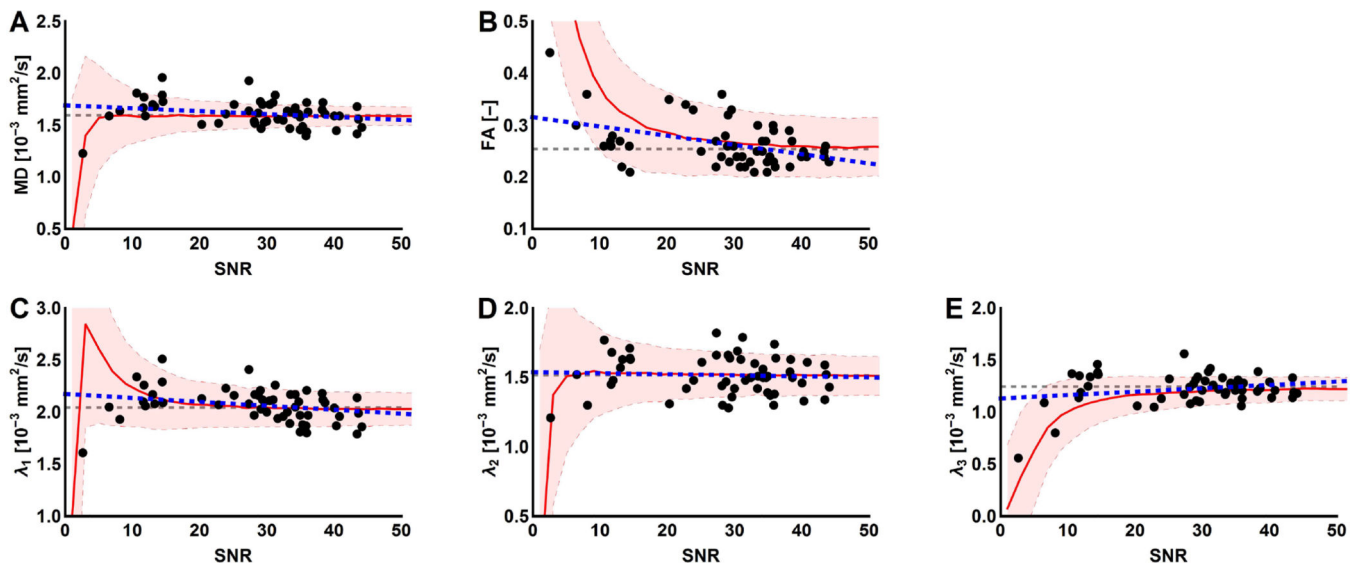


Figure 2.

Representation of the confounding effect of SNR. The individual DTI parameters are plotted against the SNR. (A–E) Each dot represents an individual muscle of a healthy control subject (black) with the corresponding fit (blue dashed line). Stabilization starts to occur in the higher SNR ranges and seems to vary between DTI parameters. In the background of the graph, the mean (red line) and standard deviation (shaded area) are shown of the DTI parameters as a function of SNR derived from the simulation experiment using WLLS. The grey dashed line indicates the true values used as input for the simulations. Clearly visible in the low SNR ranges are an overestimation of FA and an underestimation of MD and the eigenvalues.

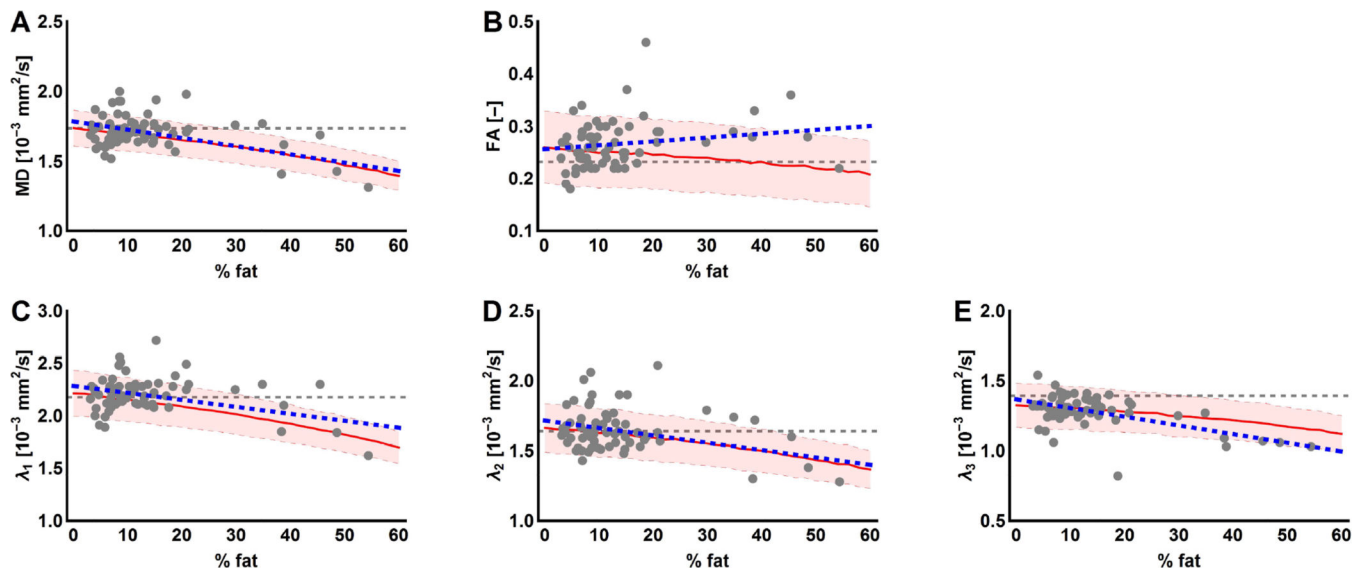


Figure 3.

Visualization of the confounding effect of infiltration of adipose tissue on the DTI parameter estimation. The individual DTI parameters are plotted against the fat fraction (%). (A–E) Each dot represents an individual muscle of a DMD patient (grey) with the corresponding fit (blue dashed line). In the background of the graph, the mean (red line) and standard deviation (shaded area) are shown of the DTI parameters as a function of %fat derived from the simulation experiment using WLLS. The grey dashed line indicates the true values used as input for the simulation experiment.

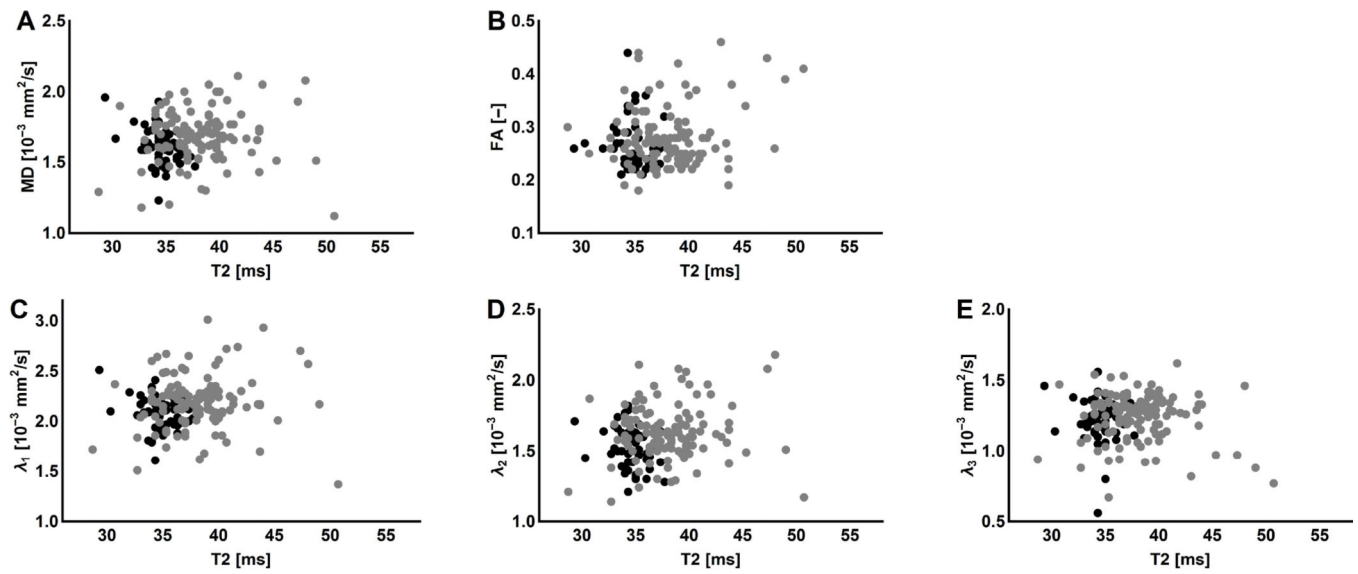


Figure 4.

The effect of T₂ changes on the DTI parameter estimation. The individual DTI parameters are plotted against the mean water T₂ values. (A–E) Each dot represents an individual muscle of a DMD patient (grey) or a healthy control subject (black). The small but significant increased mean water T₂ values in DMD patients seem to have a negligible effect on the DTI parameter estimation.

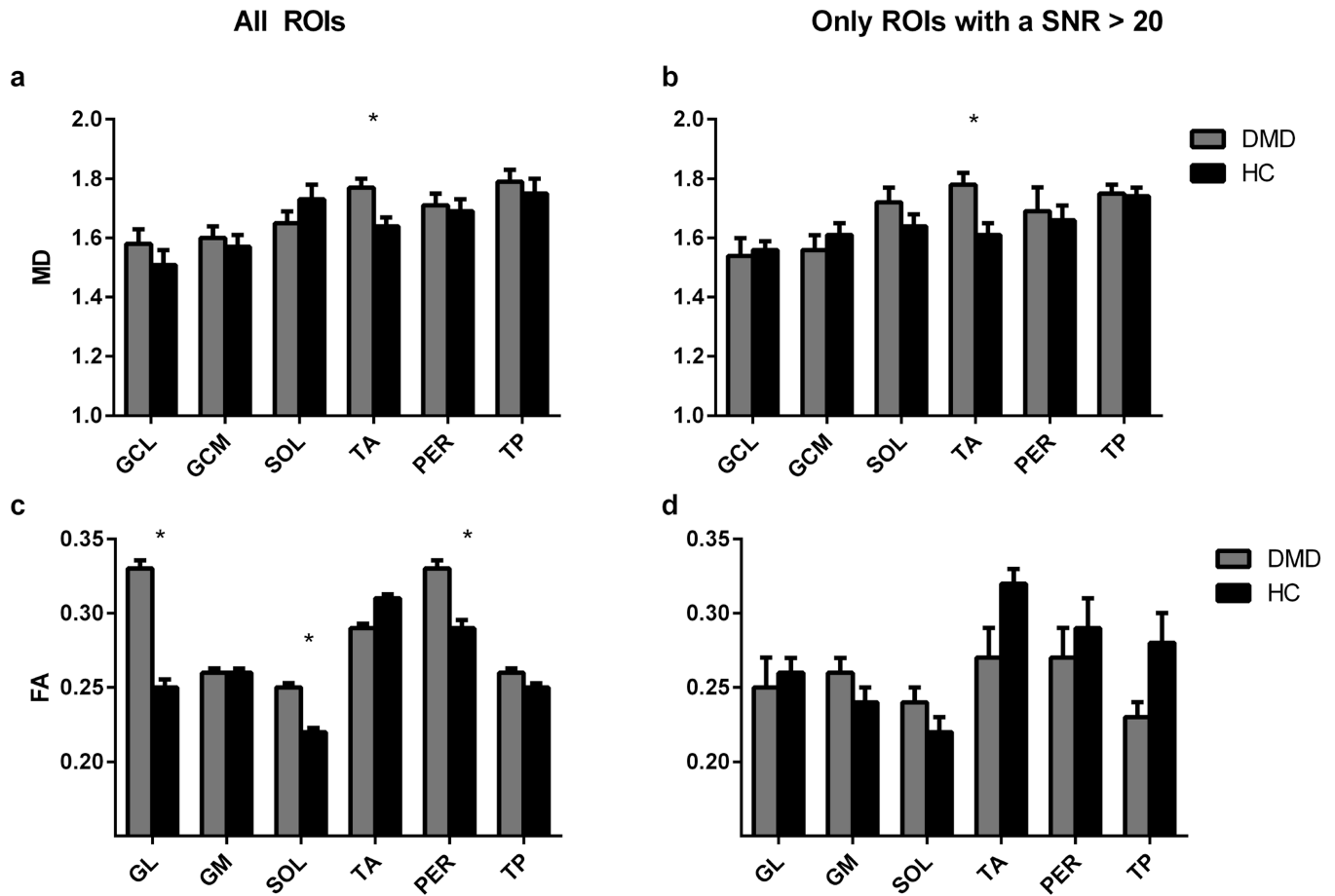


Figure 5. Mean values \pm SD of the Mean Diffusivity (A,B) and Fractional Anisotropy (C,D) using all ROIs and using only ROIs with a SNR>20 of the investigated muscles in DMD patients (grey) versus healthy control subjects (black). Muscles with values which were significantly different are marked with an asterisk (*). Remarkable is the increased FA in some of the muscles of the DMD patients using all ROIs (C), which is probably an artificial finding, since the effect disappears when low SNR data is rejected (D). (GM = medial head of gastrocnemius, GL = lateral head of the gastrocnemius, SOL = soleus, TA = anterior tibialis, PER = peroneus and TP = posterior tibialis).

Table 1Mean values \pm SD for the different DTI parameters

	Only ROIs with a SNR>20		All ROIs	
	DMD	Controls	DMD	Controls
GL	N = 4	N=9	N=16	N =12
λ_1	1.95 \pm 0.08	2.01 \pm 0.04	1.93 \pm 0.07	2.13 \pm 0.08
λ_2	1.42 \pm 0.07	1.51 \pm 0.04	1.50 \pm 0.06	1.53 \pm 0.07
λ_3	1.31 \pm 0.03* (p<0.001)	1.15 \pm 0.02	1.13 \pm 0.05	1.08 \pm 0.05
MD	1.54 \pm 0.06	1.56 \pm 0.03	1.58 \pm 0.05	1.51 \pm 0.05
FA	0.25 \pm 0.02	0.26 \pm 0.01	0.33 \pm 0.02* (p=0.04)	0.25 \pm 0.02
GM	N=7	N=10	N=16	N =12
λ_1	1.98 \pm 0.05	2.07 \pm 0.04	2.1 \pm 0.06	2.00 \pm 0.07
λ_2	1.50 \pm 0.04	1.46 \pm 0.04	1.49 \pm 0.03	1.46 \pm 0.04
λ_3	1.28 \pm 0.04	1.25 \pm 0.04	1.21 \pm 0.03	1.23 \pm 0.03
MD	1.56 \pm 0.05	1.61 \pm 0.04	1.60 \pm 0.04	1.57 \pm 0.04
FA	0.26 \pm 0.01	0.24 \pm 0.01	0.26 \pm 0.01	0.26 \pm 0.01
SOL	N=8	N=10	N=16	N =12
λ_1	2.23 \pm 0.05	1.99 \pm 0.07	2.06 \pm 0.05	2.14 \pm 0.06
λ_2	1.70 \pm 0.05	1.59 \pm 0.05	1.69 \pm 0.04	1.60 \pm 0.05
λ_3	1.31 \pm 0.04	1.32 \pm 0.03	1.28 \pm 0.03	1.32 \pm 0.04
MD	1.72 \pm 0.05	1.64 \pm 0.04	1.65 \pm 0.04	1.73 \pm 0.05
FA	0.24 \pm 0.01	0.22 \pm 0.01	0.25 \pm 0.01* (p=0.006)	0.22 \pm 0.01
TA	N=10	N=10	N=14	N =12
λ_1	2.30 \pm 0.05	2.19 \pm 0.05	2.31 \pm 0.04	2.22 \pm 0.04
λ_2	1.66 \pm 0.04	1.54 \pm 0.04	1.65 \pm 0.03	1.56 \pm 0.04
λ_3	1.33 \pm 0.03* (p<0.007)	1.17 \pm 0.03	1.31 \pm 0.03* (p=0.024)	1.2 \pm 0.03
MD	1.78 \pm 0.04* (p<0.009)	1.61 \pm 0.04	1.77 \pm 0.03* (p=0.020)	1.64 \pm 0.03
FA	0.27 \pm 0.02	0.32 \pm 0.01	0.29 \pm 0.01	0.31 \pm 0.01
PER	N=5	N=9	N=14	N =12
λ_1	2.18 \pm 0.08	2.18 \pm 0.06	2.27 \pm 0.06	2.19 \pm 0.07
λ_2	1.60 \pm 0.06	1.59 \pm 0.05	1.69 \pm 0.05	1.61 \pm 0.05
λ_3	1.25 \pm 0.05	1.23 \pm 0.04	1.12 \pm 0.04	1.22 \pm 0.05
MD	1.69 \pm 0.08	1.66 \pm 0.05	1.71 \pm 0.04	1.69 \pm 0.04
FA	0.27 \pm 0.02	0.29 \pm 0.02	0.33 \pm 0.02* (p=0.049)	0.29 \pm 0.02
TP	N=12	N=10	N=14	N =12
λ_1	2.18 \pm 0.05	2.18 \pm 0.06	2.31 \pm 0.04	2.25 \pm 0.05
λ_2	1.67 \pm 0.04	1.66 \pm 0.04	1.7 \pm 0.04	1.68 \pm 0.04

	Only ROIs with a SNR>20		All ROIs	
	DMD	Controls	DMD	Controls
λ_3	1.35±0.03	1.36±0.03	1.38±0.03	1.37±0.03
MD	1.75±0.03	1.74±0.03	1.79±0.04	1.75±0.05
FA	0.23±0.01	0.28±0.02	0.26±0.01	0.25±0.01

(FA: fractional anisotropy, MD: mean diffusivity and the eigenvalues (λ_1 , λ_2 , and λ_3)) using all ROIs and using only ROIs with a SNR>20 in healthy controls and DMD patients of the investigated muscles (medial and lateral head of gastrocnemius (GM, GL), soleus (Sol), anterior tibialis (TA), peroneus (PER) and posterior tibialis (TP)).

Significant differences between patients and controls are marked with an asterisk (*).